Optical investigations of defects in $Cd_{1-x}Zn_xTe$

W. Stadler, D.M. Hofmann, H.C. Alt, T. Muschik, and B.K. Meyer
Physik-Department E16, Technische Universität München, James-Franck-Strasse, D-85747 Garching, Germany

E. Weigel and G. Müller-Vogt
Kristall- und Materiallabor der Fakultät für Physik, Universität Karlsruhe, Engesserstrasse 7, D-76128 Karlsruhe, Germany

M. Salk, E. Rupp, and K.W. Benz
Kristallographisches Institut, Universität Freiburg, Hebelstrasse 25, D-79104 Freiburg, Germany
(Received 8 November 1994)

We investigated the optical properties of defects in CdTe and $Cd_{1-x}Zn_xTe$ ($0 < x < 1$). Residual impurities give rise to specific far infrared absorptions, while metal vacancy-donor complexes (A centers), identified by optically detected magnetic resonance, are characterized by their near infrared (1.4 eV) photoluminescence (PL) properties. The specific zero-phonon-line positions and phonon couplings are worked out for these complexes involving different group-VII (F,Cl,Br,In) or group-III (In,Al) donors. In addition to the A center PL two emission bands are found at 1.135 and at 1.145 eV. The temperature dependences of the PL show that the 1.145 eV luminescence follows the temperature dependence of the band gap, while the energy position of the 1.135 eV emission shifts to higher energies with increasing temperature. The A-center PL and the luminescence bands at 1.1 eV are investigated throughout the complete alloy composition range from $x = 0$ to 1. The A center and the 1.135 eV band were found to follow the band-gap shift from CdTe to ZnTe, whereas the 1.145 eV luminescence keeps its emission energy constant.

I. INTRODUCTION

Generally only one type of conductivity is easily achieved in wide band-gap II-VI semiconductors[1] (n type, with the exception of ZnTe, which is the most commonly obtained p type[2]). To convert the conductivity type and thus to be able to form p-n junctions remains a difficult task. It requires either highly sophisticated growth techniques for phase equilibrium growth at high temperatures, or epitaxial growth working at temperatures far below.[3–5]

Early theories to explain these phenomena quoted self-compensation, i.e., the formation of intrinsic defects which compensate the dopants, to be the origin of this behavior.[6–9] But recent calculations showed that intrinsic defects play only a minor role for growth under equilibrium conditions,[10] and the poor solubility of the doping elements was made responsible.[11–13]

The situation seems to be somehow better in CdTe ($E_{gap} = 1.606$ eV at $T = 4.2$ K); it can be made p and n type by appropriate doping. But surprisingly high resistive ($> 10^8$ Ω cm, p-type) crystals are commonly obtained by n-type doping. As these crystals are usually grown under Te-rich conditions, the self-compensation model is used to explain this behavior: Cadmium vacancies (V_{Cd}) are thought to be present, which act as deep double acceptors, or form complexes with the dopants (A centers, V_{Cd}-donor pair defects, single acceptors).

However, it took over 40 years to show unambiguously that these defects really do exist in CdTe. Meanwhile, Te as well as Cd vacancies have been identified by electron paramagnetic resonance (EPR) (Refs. 14 and 15) and A centers by optically detected magnetic resonance (ODMR).[16,17] One result was that A centers contribute to the 1.4 eV emission band. Emission in this spectral range was extensively studied[18] and it turned out that residual impurities such as copper, silver, and gold can give rise to photoluminescence (PL) bands in this spectral region. This makes a specific identification of the defects from PL measurements alone quite difficult.

But in view of the electrical properties, i.e., high resistivity CdTe, both A centers and residual impurities (Cu, Ag, Au) cannot explain the experimental results due to their rather shallow level positions being located between 100 and 250 meV above the valence band (VB).

Much less is known about the optical and electrical properties of the Te and Cd vacancies. Photo-EPR experiments indicate the $V_{Te}^{0/+}$ level to be at 200 meV above the valence band, and $\leq$ 400 meV for the $V_{Cd}^{2-/-}$ level. To get further insight into the compensation of the material thus requires paying special attention to deep defects (deep center luminescence).

In ZnTe the dominant residual impurities, Cu and Ag, have very similar properties to CdTe. Also A centers, at least for the case of the A center involving group-III (Al) donors, behave very similarly (level position: $E_{VB} + 190$ meV).[19] Anion and cation vacancies are not identified in ZnTe so far. Thus, the compensation mechanism, which renders the material to be p type, is still unknown.

The outline of the paper is as follows. First, we will describe the PL and infrared absorption properties of the dominant residual impurities (Cu, Ag) in CdTe and ZnTe. The infrared absorption is the most specific tool

 ©1995 The American Physical Society

to characterize these defects. It is followed by a detailed study of the donor-acceptor-pair (DAP) PL band of A centers in CdTe involving group-III and group-VII donors. The correlation to the PL is based on the ODMR experiments presented in the proceeding paragraph. The specific differences in zero-phonon-line (ZPL) position and phonon coupling will be worked out for the A centers involving six different, either group-VII or group-III, donors.

In addition to these PL bands, emissions at lower energies (1.0 – 1.2 eV) are detected. The temperature dependent PL experiments reveal that the peak position of a 1.145 eV band decreases similarly to the band gap of CdTe, while the peak position of an emission at 1.135 eV increases in energy as a function of temperature. This behavior is described within the configuration coordinate model as being caused by an internal defect transition.

The properties of the shallow as well as the deep PL bands were investigated for a series of $Cd_{1-x}Zn_xTe$ samples covering the complete alloy composition range. It enables us to attribute a PL band at about 2.2 eV as being due to chlorine A centers in ZnTe.

Summarizing the experimental results for the A centers and the Cd and Te vacancies in other II-VI semiconductor host crystals, the expected properties of these defects in CdTe and ZnTe will be discussed and compared with the properties of the PL bands found in the $Cd_{1-x}Zn_xTe$ system.

II. EXPERIMENTAL DETAILS

The CdTe samples investigated were grown either by the vertical Bridgman technique or by the traveling heater method (THM).[20,21] For both methods, in a first step, polycrystalline CdTe was synthesized using $6N$ Cd and $6N$ Te in a stochiometric ratio. To achieve n-type doping elements of group III (Al, In) and group VII (F, Cl, Br, I) were added. For fluorine and iodine doping their corresponding cadmium halides were used, while for doping with the group-III elements as well as for doping with bromine, the elemental forms were used. In the case of chlorine both, the elemental form and $CdCl_2$ was taken. The dopants in a concentration of 10^{17} – 10^{20} cm^{-3} were added either to the polycrystalline CdTe in vertical Bridgman runs or to the tellurium zone in the THM. With both techniques, the crystal growth was carried out under Te excess: Using the vertical Bridgman technique, the crystals were grown on the Te-rich side of the phase diagram, while for the THM a Te zone was used. The growth rate was in any case about 0.5 mm/h, with temperature gradients of typically 10 K/cm. The rate for cooling down to room temperature was about 10 K/h.

The ternary $Cd_{1-x}Zn_xTe$ crystal was grown with the THM from an (111) oriented undoped $Cd_{0.96}Zn_{0.04}Te$ seed, with a reservoir consisting of ZnTe and CdTe, each doped with 2×10^{19} cm^{-3} Cl. Again a Te zone was used to guarantee Te rich growth. Under these conditions, a crystal was obtained containing almost the complete composition range from $x = 0$ to $x = 1$. For the experiments it was cut into 19 slices, the Zn contents were determined by energy dispersive analysis of x rays (EDX) as well as by analyzing the excitonic PL spectrum using the energy gap dependence of the composition. The band gap energy was estimated with $E_{gap} = E_{(X,A^0)} + 17$ meV, where $E_{(X,A^0)}$ is the position of the principal acceptor bound exciton. The compositions of the slices were calculated using the formula given by Reno and Jones,[22]

$$E_{gap} = (1.606 + 0.322x + 0.463x^2)\ \text{eV} . \quad (1)$$

The EDX technique and analysis of the excitonic line position lead within the experimental error to the same results for the composition.

To carry out the PL measurements the samples were placed in an Oxford cryostat, allowing variable temperatures from 1.6 to 300 K. The luminescence was excited by the 488 nm line of an Ar^+ ion laser (Spectra Physics 164), with an output power up to 2 W. The spectral dependence of the emission was analyzed by a Jarrell-Ash 25–100 1 m high resolution double monochromator (f 1:8.7) and detected either by a photomultiplier or by a LN_2 cooled North Coast EO-817L germanium detector.

For the time-resolved luminescence experiments the emission was excited by 700 ps pulses from a nitrogen laser pumped dye laser. The decay of the luminescence was recorded by a S1 photomultiplier and a digital oscilloscope. The time resolution of the apparatus is 2 ns.

The experimental setup for the ODMR is described elsewhere.[16] The Fourier transform infrared experiments were performed on a commercial Bruker IFS 113v spectrometer.

III. RESULTS

A. Residual impurities in undoped CdTe and ZnTe

It is well known[23,24] that undoped CdTe and ZnTe crystals can contain impurities in a concentration range up to 10^{17} cm^{-3}. Some of these impurities such as copper or silver are already present in the starting materials as contamination, while others (e.g., Na, Ca, Li) were introduced unintentionally to the crystal during growth from the apparatus.

In the undoped samples investigated, the dominant residual impurities are copper and silver. Both elements act as rather shallow acceptors and are well characterized by infrared absorption spectra. Typical spectra are shown in Figs. 1 and 2. In CdTe (Fig. 1) in the spectral range from 1000 cm^{-1} to 1200 cm^{-1}, the hydrogen-like effective mass transitions of copper are located. The low energy $1S_{3/2} \rightarrow 2P_{5/2}(\Gamma_8)$ line is at $E = 130.94$ meV.[25] Up to 5 additional transitions are observed, their energetic positions are listed in Table I. The fourth column gives the energy difference to the copper binding energy of $E_{1S_{3/2}} = 146$ meV.[26] The assignment to the respective transition (column 5) is based on the theory of Baldereschi and Lipari.[27] With the valence band parameters for CdTe (effective Rhydberg energy $R_0 = 30$ meV, spin orbit interaction $\mu = 0.69$, and cubic contribution $\delta = 0.12$) this theory leads very accurately to the values

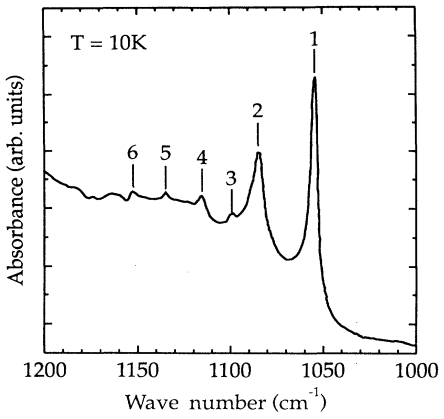

FIG. 1. Far infrared absorption spectrum of copper in CdTe. Absorption lines labeled 1–6 are identified to be due to the hydrogenlike effective mass transition of the copper acceptors (see text).

TABLE I. Energy positions of the hydrogenlike effective mass transitions of Cu and Ag acceptor in CdTe and ZnTe, respectively. The $1S_{3/2}$ ground-state energy $E_{1S_{3/2}}$ of the acceptor was taken as 146.0 meV for Cu_{Cd} and as 123.0 meV for Ag_{Zn}.

Defect	No.	Energy E (meV)	$E_{1S_{3/2}} - E$ (meV)	Transition
Cu_{Cd}	1	130.94	15.06	$1S_{3/2} \rightarrow 2P_{5/2}(\Gamma_8)$
	2	134.60	11.40	$1S_{3/2} \rightarrow 2P_{5/2}(\Gamma_7)$
	3	136.38	9.62	$1S_{3/2} \rightarrow 3P_{3/2}$
	4	138.33	7.67	$1S_{3/2} \rightarrow 3P_{5/2}(\Gamma_8)$
	5	140.64	5.36	$1S_{3/2} \rightarrow 3P_{5/2}(\Gamma_7)$
	6	142.65	3.35	$1S_{3/2} \rightarrow 2P_{1/2}$
Ag_{Zn}	1	105.9	17.1	$1S_{3/2} \rightarrow 2P_{5/2}(\Gamma_8)$
	2	109.8	13.2	$1S_{3/2} \rightarrow 2P_{5/2}(\Gamma_7)$
	3	113.4	9.6	$1S_{3/2} \rightarrow 3P_{3/2}$
	4	115.1	7.9	$1S_{3/2} \rightarrow 3P_{5/2}(\Gamma_8)$
	5	116.4	6.6	$1S_{3/2} \rightarrow 3P_{5/2}(\Gamma_7)$
	6	117.2	5.8	$1S_{3/2} \rightarrow 2P_{1/2}$

for the $1S_{3/2} \rightarrow 2P_{5/2}$ transition and to the splitting of the $2P_{5/2}$ state.

With these valence band parameters one can expect that the $2P_{1/2}$ energy level of Cu in CdTe should be 3.8 meV above VB. Indeed we found a peak (No. 6) with $E_{1S_{3/2}} - E_6 = 3.35$ meV, close to the theoretically predicted value. Therefore, we attribute the peak with the highest energies (No. 6) to the $1S_{3/2} \rightarrow 2P_{1/2}$ transition. Because it is known that the oscillator strength of the $1S_{3/2} \rightarrow 2P_{3/2}$ transition is very low compared to the oscillator strength of the $1S_{3/2} \rightarrow 2P_{5/2}$ transition,[28] this transition is not observable, but should be at $E_{1S_{3/2}} - E = 22.9$ meV in CdTe.

The theory of Baldereschi and Lipari does not include the $n = 3$ states of the shallow acceptors, but following the arguments given in the paper we can assign the three remaining transitions at $E - E_{1S_{3/2}} = 9.6$ meV (No. 3), 7.7 meV (No. 4), and 5.4 meV (No. 5) in CdTe to the $1S_{3/2} \rightarrow 3P_{3/2}$, $1S_{3/2} \rightarrow 3P_{5/2}(\Gamma_8)$, and $1S_{3/2} \rightarrow 3P_{5/2}(\Gamma_7)$ transition, respectively.

A similar analysis was performed for the infrared absorption of silver in ZnTe (Fig. 2 and second part of Table I) with band parameters[2] $R_0 = 40.6$ meV, $\mu = 0.58$, and $\delta = 0.15$ and a binding energy of 123 meV. Again, up to six transitions could be identified. In addition, the LO ($\hbar\omega = 26.2$ meV) phonon replica of these transitions can be seen in Fig. 2 above 1050 cm^{-1}.

In photoluminescence, copper gives rise to a characteristic excitonic line at $E = E_{gap} - 16.98$ meV in CdTe, the exciton bound to the neutral copper acceptor.[29] In addition a DAP band is observed in the spectral range from approximately 1.2 eV to 1.5 eV (Fig. 3). The emis-

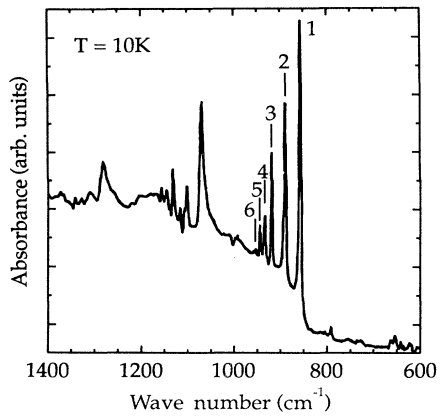

FIG. 2. Far infrared absorption spectrum of silver in undoped ZnTe. Absorption lines labeled 1–6 are identified to be due to the hydrogenlike effective mass transition of the silver acceptors (see text). Lines above 1050 cm^{-1} are phonon replicas to lines 1 – 6.

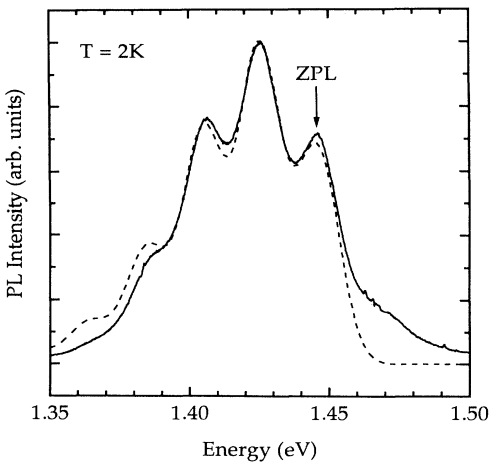

FIG. 3. Photoluminescence spectrum of the shallow donor-copper acceptor pair recombination in CdTe. The dashed line corresponds to a fit using Eq. (2) with a binding energy $E_B = 146$ meV and a Huang-Rhys parameter $S = 1.6$.

sion consists of a zero phonon line (ZPL) followed by four phonon replicas, each separated by a phonon energy $\hbar\omega$ of approximately 21 meV. The intensity of the nth phonon replicas can be described by a Poisson distribution,

$$I(n) = I_0 e^{-S} \frac{S^n}{n!}, \tag{2}$$

with the Huang-Rhys coupling parameter S and a constant factor I_0. The total shape of the emission can be simulated by a Poisson distribution combined with Gaussian lines for each individual line. Although it is known that the line shape in a DAP transition shows distinct deviations from a Gaussian line,[30] this simple estimate fits the experimental data quite well (dashed line in Fig. 3). A best fit was obtained for $E_B = 146$ meV and $S = 1.6$ and agrees with the established values for Cu. It has to be pointed out that in this spectral range at least two other emissions can appear, the so-called D line[31] as well as the DAP recombination of the A centers (see below), which have similar line shapes and binding energies.

For ZnTe the Cu binding energy is 149 meV,[2] almost the same as in CdTe, and also the A centers and the D-line emissions appear in the same spectral range. For Ag in CdTe E_B was determined to 107 meV,[25] while this value in ZnTe is $E_B = 123$ meV. In both semiconductors the phonon coupling is $S \approx 0.1 - 0.2$, much smaller compared to copper or A centers.

B. Photoluminescence of the *A* centers in CdTe

In the previous section, it was shown that the residual impurities give rise to luminescence in the spectral range from 1.3 – 1.5 eV. In n-type doped material, the DAP recombination in this spectral range is much more intense. It was historically called the 1.4 eV band.[32] The details of this band, such as the position of the ZPL and the phonon coupling depend on the chemical nature of the involved donors and are worked out in this section. The acceptors involved are A centers for which a detailed structure analysis will be given in Sec. III C.

Figure 4 shows two examples of the 1.4 eV band for bromine- and indium-doped CdTe. As can be seen, the spectra differ in ZPL positions and intensity distribution. The calculated spectra using Eq. (2) are drawn as dashed lines. The values obtained for S, $\hbar\omega$, and E_B for all dopants are listed in Table II. The binding energies of the acceptors involved are calculated with

$$E_{\mathrm{ZPL}} = E_{\mathrm{gap}} - E_B - E_D + \frac{e^2}{4\pi\epsilon_r\epsilon_0|\vec{r}|}, \tag{3}$$

neglecting the last term, which describes the Coulombic interaction. This simplification is valid for low doping concentrations only, and we assume a donor binding energy of 14 meV [value obtained by the effective mass theory (EMT)].[33] The 1.4 eV band was found in each n-doped sample. The intensity distributions as well as the binding energies are different for different dopants.

Temperature dependent PL measurements were performed in a range from $T = 1.6$ K to $T = 125$ K. At temperatures above 70 K, the structures are washed out and at $T > 125$ K the emission was too weak to be detected. In Fig. 5 the normalized PL intensity of an In-doped sample is shown as a function of the temperature. The quenching behavior of the PL intensity $I(T)$ is described by the expression

$$\frac{I(T)}{I_0} = \frac{1}{1 + c_1 e^{-E_1/k_B T} + c_2 e^{-E_2/k_B T}}, \tag{4}$$

with the constants c_1 and c_2 and two activation energies E_1 and E_2. An attempt to model the experimental data with one activation energy only failed. For the best fit, we obtain the parameters $c_1 = 3 \pm 0.2$, $c_2 = (1.5 \pm 0.1) \times 10^6$, $E_1 = (5 \pm 1)$ meV, and $E_2 = (95 \pm 10)$ meV. It is obvious to attribute the smaller activation energy to the donor ionization energy (≈ 14 meV) and the larger one to the acceptor binding energy (≈ 142 meV). These results are the first evidence that we are dealing with a DAP transition. Similar behavior with only slightly different values for E_1 and E_2 are found for the other dopants.

In Fig. 6, the position of the ZPL is shown as a function of temperature. The position shifts towards higher

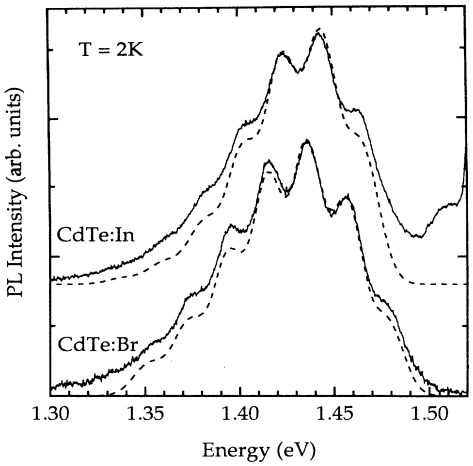

FIG. 4. Photoluminescence spectra of A centers in bromine- and indium-doped CdTe. The dashed lines give the calculated line shapes (for details see text).

TABLE II. Binding energy (E_B) and Huang-Rhys coupling parameters S of cation vacancy-donor centers (A centers) involving different donor species.

Donor	Group	E_B (meV)	S	$\hbar\omega$ (meV)
F	VII	116	3.2	20.9
Cl	VII	125	2.2	20.6
Br	VII	119	2.6	20.0
I	VII	128	1.5	19.2
Ga	III	131	1.7	20.9
In	III	142	1.8	20.5

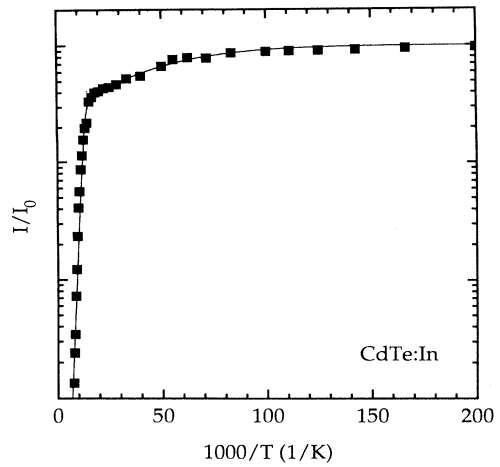

FIG. 5. Temperature dependence of the In A-center luminescence in indium-doped CdTe. The drawn line represents a fit with two binding energies of 5 and 90 meV.

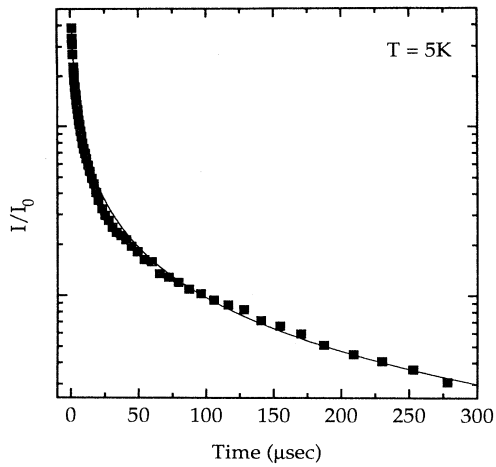

FIG. 7. Time decay of the bromine A-center emission in CdTe. The drawn line represents a fit according to Eq. (6).

energies until it reaches a maximum at $T \approx 30$ K. For higher temperatures it decreases linearly with a slope of $(2.9 \pm 0.2) \times 10^{-4}$ eV/K, in very good agreement with the temperature dependence of the band gap of CdTe $dE/dT = 3 \times 10^{-4}$ eV/K.[34] The behavior is explained by the change from a DAP transition to a free to bound recombination. A complete theoretical analysis was given in Biernacki *et al.*[35]

The time decay of the A-center luminescence in a bromine-doped CdTe bulk sample is given in Fig. 7. If the origin of the luminescence was of a free to bound type, a monoexponential time decay is expected. From Fig. 7 it is obvious that the time decay is nonexponential. The probability $W(|\vec{r}|)$ for the recombination of a hole and an electron at a distance $|\vec{r}|$ is given by[36]

$$W(|\vec{r}|) = \frac{1}{\tau} = W_{\max} e^{-2|\vec{r}|/a_0} \ . \qquad (5)$$

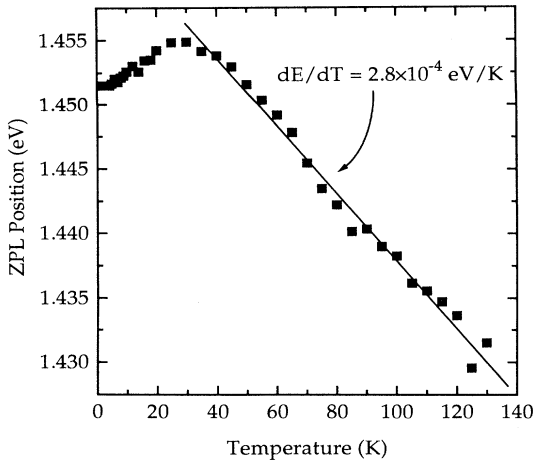

FIG. 6. Temperature dependence of the zero phonon line peak position of indium A centers in CdTe.

$W_{\max}$ is the maximum transition probability for $|\vec{r}| \to 0$, it corresponds to the time decay at $t = 0$ and is, therefore, a material dependent constant. a_0 is the Bohr radius for the weaker bound particle, i.e., the Bohr radius of the donor electron ($a_0 \approx 50$ Å). For a DAP transition, there exist different distances $|\vec{r}|$ and, therefore, a distribution of lifetimes. If either the donor or the acceptor concentration dominates in the sample, the luminescence intensity as a function of time is given by the formula from Thomas *et al.*:[36]

$$I(t) = \left\{ 4\pi N \int_0^\infty W(|\vec{r}|) e^{-W(|\vec{r}|)t} r^2 dr \right\} \times \left\{ \exp\left[4\pi N \int_0^\infty \left(e^{-W(|\vec{r}|)t} - 1 \right) r^2 dr \right] \right\}, \qquad (6)$$

with N the number of particles and $W(|\vec{r}|)$ from Eq. (5). The intensity distribution $I(t)$ according to Eq. (6) was calculated for the complete measured time scale. A best fit was obtained with $N \approx 10^{16}$ cm^{-3} and $W_{\max} \approx 3 \times 10^7$ s^{-1}. Taking into account a doping concentration of 10^{19} cm^{-3} bromine, the value of N leads to a segregation coefficient of about 10^{-3}. This value was supported by results of Hall measurements.[20,21,37] For $W_{\max}$ in CdTe there is to our knowledge no value in the literature, but a comparison with other II-VI materials [ZnSe (Ref. 38): $1.5 \times 10^8 - 2.8 \times 10^9$ s^{-1}, CdS (Ref. 38): 4×10^8 s^{-1}] shows reasonable agreement.

C. ODMR on the A centers in CdTe

The identification of the acceptors responsible for the 1.4 eV PL band is based on the optically detected magnetic resonance results, briefly described in this section. A more detailed description can be found in Ref. 16 and Ref. 17.

The rotation patterns of the observed acceptor resonances are shown in Fig. 8(a) for CdTe:Cl and in Fig. 8(b)

for CdTe:In. Clearly, two different patterns are observed. To analyze these rotation patterns, the appropriate spin Hamiltonian was used:[19,39]

$$\mathcal{H} = \tilde{g}\mu_B \vec{B}\vec{S} + \vec{S}\tilde{A}\vec{I}, \quad \tilde{g} = \begin{pmatrix} g_{xx} & 0 & 0 \\ 0 & g_{yy} & 0 \\ 0 & 0 & g_{zz} \end{pmatrix}, \qquad (7)$$

with the g tensor $\tilde{g}$, the spin matrix $\vec{S}$, the hyperfine interaction tensor $\tilde{A}$, and the nuclear spin vector $\vec{I}$. In the case of the chlorine A center the $\tilde{g}$ tensor turned out to have trigonal symmetry, resulting in a g tensor $\tilde{g}$ with the components $g_{xx} = g_{yy} = g_\perp$ and $g_{zz} = g_\parallel$. The In A center is of lower symmetry, the angular dependence could be described accurately by monoclinic symmetry. The different symmetries correspond very well to the models proposed for the A centers: The A center consists of a cadmium vacancy and a donor located on the nearest (a group-VII element substitutes a tellurium atom) or on the next-nearest (a group-III element substitutes a cadmium atom) lattice site (Fig. 9), resulting in either trigonal or monoclinic symmetry.

These models are further confirmed by the observation of the ligand hyperfine interaction with the neighboring Te nuclei. This interaction results in satellite lines, which

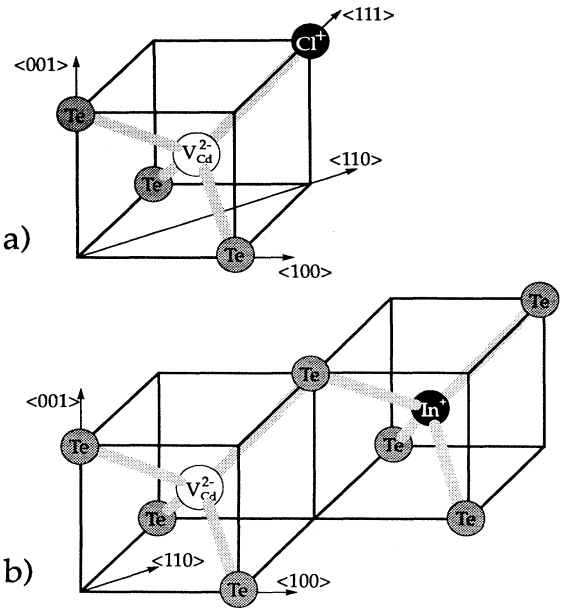

FIG. 9. Models of the A centers in CdTe, (a) involving a chlorine (group VII) and (b) involving an indium (group III) donor.

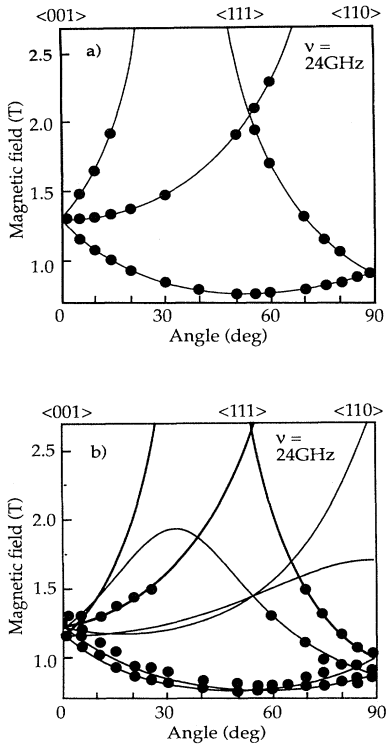

FIG. 8. Angular dependence of the A-centers resonances observed by optically detected magnetic resonance. (a) A center in chlorine-doped CdTe. (b) A center in indium-doped CdTe. The samples are rotated in a (110) plane, 90° from a ⟨001⟩ towards a ⟨110⟩ crystal axis.

accompany each of the strong resonances (Fig. 10). The intensity of the satellite lines depends on the statistical occupation of the nearest-neighbor lattice sites by $^{123/125}$Te isotopes, which carry nuclei spin $I = \frac{1}{2}$ (abundance 8%, all other Te isotopes have $I = 0$). In case of the In A center (compare Fig. 9), we have to take four nearest-neighbor lattice sites into account, which results in an intensity ratio of 6 : 1 for the central line compared to the two satellite lines shown in Fig. 10 (additional satellite lines are expected;[39] however, with an intensity

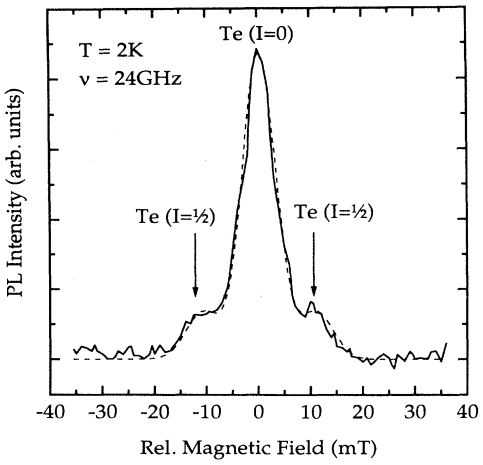

FIG. 10. Hyperfine splitting of the A-center resonances in CdTe:In, due to the interaction with the Te neighbors.

TABLE III. Comparison of A-centers properties in II-VI compounds.

II-VI compound	CdTe		ZnTe		ZnSe	ZnS
Dopant	Cl	In	Cl	Al	Cl	I
E_B (meV)	120	140	155	190	500	≈ 1000
g values	$g_{\parallel} = 2.2$	$g_{xx} = 1.00$	$g_{\parallel} = 2.66$	$g_{xx} = 0.22$	$g_{xx} = 2.22$	$g_{\parallel} = 2.005$
	$g_{\perp} = 0.4$	$g_{yy} = 0.35$	$g_{\perp} = 0$	$g_{yy} = 0.27$	$g_{yy} = 2.19$	$g_{\perp} = 2.075$
		$g_{zz} = 2.23$		$g_{zz} = 2.54$	$g_{zz} = 1.95$	
hyperfine interaction (cm^{-2})	2.7×10^{-2}	1.9×10^{-2}	1.9×10^{-2}	1.8×10^{-2}	2.5×10^{-2}	
Refs.	16	17	19	19	40	40

much too low to be observed in our experiment). The experimental observation 6.5 : 1 is thus in good agreement. In case of the chlorine A center, only three Te neighbors are present (one Te site is occupied by the donor, see Fig. 9). Thus, the intensity ratio is expected to be 8 : 1, as indeed observed.[16]

The g values and the hyperfine constants found in the ODMR experiments are listed in Table III in comparison to the values for A centers in other II-VI compounds. The A centers in II-VI compounds can be divided into two groups: (a) the A centers in ZnSe and ZnS. They are deep defects, with large binding energies of about 500 meV in ZnSe and 1000 meV in ZnS.[40] The g values differ only slightly from the g value of the free electron $g = 2$, typical properties of deep defects. In contrast to these defects, the A centers in CdTe and ZnTe are shallow or at least intermediate deep defects. The binding energies are below 200 meV and the g values strongly differ from $g = 2$.

Although the A centers in the II-VI compounds can be divided into deep and shallow defects from the energy level point of view, the hyperfine constants as an additional signature are in all cases nearly the same. Up to now, to our knowledge, there has been no theoretical explanation for this behavior.

D. Photoluminescence on deep centers in CdTe

The origin of the known deep luminescence bands in CdTe is less established. Lischka *et al.* correlated broad luminescence bands centered at 1.1 eV to a defect recombination involving iron,[41] the bands were labeled FE1030 and FE1130. Similar emissions were observed by Bowman and Cooper in iron implanted CdTe samples.[42]

In undoped as well as in doped CdTe samples, we observe a luminescence band at 1.135 eV, in some samples a second band at 1.145 eV (Fig. 11). Because both emissions have full widths at half maximum (FWHM) of 100 – 200 meV and the peak positions are close in energy, the separation of the luminescence bands by steady-state PL is very difficult and temperature dependent PL measurements may give further insight.

For the 1.145 eV band, the FWHM and the peak position as a function of the temperature are shown in Fig. 12. The FWHM stays constant up to 50 K and increases with higher temperatures. This behavior can be described in a single configuration coordinate diagram:[43]

$$\mathrm{FWHM}(T) = 2.36\sqrt{S}\hbar\omega_{\mathrm{phonon}}\sqrt{\coth\frac{\hbar\omega_{\mathrm{phonon}}}{2k_BT}}, \quad (8)$$

where the symbols have their common meaning. A best fit according to Eq. (8) was obtained with values of $S = 7.1 \pm 0.3$ and $\hbar\omega_{\mathrm{phonon}} = (14.6 \pm 0.5)$ meV (drawn line in Fig 12). Within the configuration coordinate model the position of the nonresolved ZPL should be at $E_{\mathrm{ZPL}} = (1.25 \pm 0.02)$ eV (peak position plus $S\hbar\omega$). Assuming a free to bound transition, the binding energy of the defect is estimated to be $E_B = E_{\mathrm{gap}} - E_{\mathrm{ZPL}} = (350 \pm 20)$ meV.

The peak energy shifts with increasing temperatures to lower energies, i.e., it shows a similar behavior to the band gap. The temperature gradient was determined to be $dE/dT = (1.8 \pm 0.4) \times 10^{-4}$ eV/K.

For comparison, the same data set for the luminescence at 1.135 eV is shown in Fig. 13. The behavior

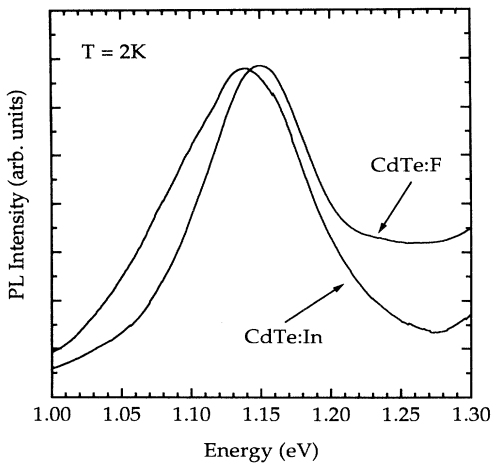

FIG. 11. Two characteristic spectra of deep luminescence bands in CdTe. In the F-doped sample the peak position is 1.135 eV and in the In-doped sample 1.145 eV.

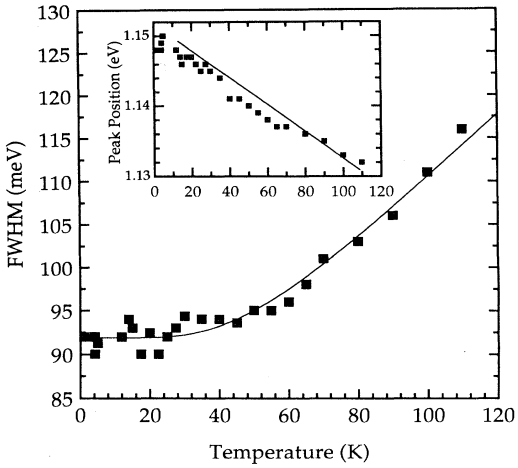

FIG. 12. Temperature dependence of the full width at half maximum (FWHM) and the peak energy (inset) of the 1.145 eV PL band in CdTe.

for the FWHM is very similar to the 1.145 eV emission. Fitting the data with the expression Eq. (8) leads to $S = 12.5 \pm 0.5$ and $\hbar\omega_{\text{phonon}} = (15.2 \pm 0.5)$ meV. With the same assumptions used above, the binding energy was estimated to $E_B = (280 \pm 15)$ meV.

The important difference to the 1.145 eV luminescence is the behavior of the peak position, which with increasing temperatures shifts to higher energies. For such a case, Shionoya *et al.*[44] showed that the peak energy of the emission E_{em} within the configuration coordinate diagram model is a linear function of the temperature:

$$E_{\text{em}}(T) - E_{\text{em}}(T=0) = \left(\frac{\nu_g^2 - \nu_e^2}{\nu_e^2} + \frac{8\nu_g^4}{\nu_e^2\left(\nu_g^2 + \nu_e^2\right)} \right) \times \left(\frac{E_{\text{ab}}(0) - E_{\text{em}}(0)}{E_{\text{em}}(0)} \right) k_B T, \tag{9}$$

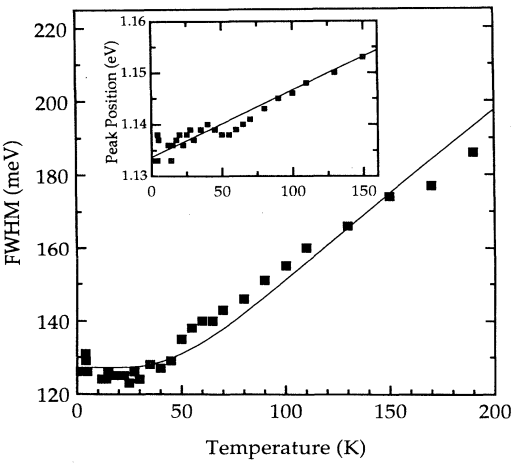

FIG. 13. Temperature dependence of the full width at half maximum (FWHM) and the peak energy (inset) of the 1.135 eV PL band in CdTe.

where $h\nu_g$ and $h\nu_e$ are the phonon energies of the ground and the excited state, respectively. $E_{\text{ab}}(0)$, the maximum absorption at $T \rightarrow 0$ was measured by photoluminescence excitation spectroscopy:[45] $E_{\text{ab}} = (1.55 \pm 0.01)$ eV at $T = 1.8$ K. $E_{\text{em}}(0)$, the peak energy of the emission at $T \rightarrow 0$ was taken to 1.135 eV from the PL experiments. With $h\nu_g = 15$ meV and $h\nu_e = 14$ meV, we can almost perfectly describe the experimental data (drawn line in Fig. 13).

The temperature dependence of the 1.145 eV PL band is typical for a free to bound or a DAP transition, whereas that of the 1.135 eV band points to an internal transition of a deep defect. In addition, further broad emission bands centered at 0.79 eV, 1.03 eV, and 1.17 eV are found in some special cases, but in intensities too weak to allow more detailed experiments.

E. PL on $Cd_{1-x}Zn_xTe$

In aluminum-doped ZnTe, a PL band at $E \approx 2.16$ eV was identified by Bittebierre and Cox by ODMR as a DAP with the Al A center.[19] In the same work, the chlorine A-center was identified, but the ODMR was observed on a recombination involving a deep luminescence band, obviously via a shunt path process. It was, therefore, our interest to study the chlorine A-center luminescence in the ternary alloy $Cd_{1-x}Zn_xTe$ and to conclude about its location in ZnTe ($x = 1$).

A selection of five representative PL spectra for samples with different Zn composition x is shown in Fig. 14. Each spectrum can be divided into three different parts:

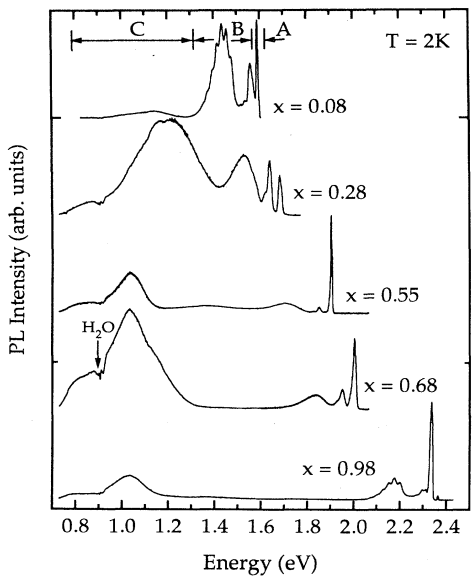

FIG. 14. Typical photoluminescence spectra observed in chlorine-doped $Cd_{1-x}Zn_xTe$ for different compositions x. The structure observed on the low energy side of the spectra are due to atmospheric water.

The sharp lines near the band edge ($E_{gap} < E < E_{gap} - 25$ meV) are due to excitonic recombinations (labeled as part A in Fig. 14), not considered further. The PL in the second range (part B, $E_{gap} - 25$ meV $< E < E_{gap} - 200$ meV) has its origin in free-to-bound or donor-acceptor-pair recombinations involving shallow acceptors with binding energies $E_b < 180$ meV. In this spectral region a broad luminescence, which shows a well resolved structure in the samples with extreme x values ($x \approx 0$ and $x \approx 1$) is observed. It is the A-center luminescence (squares in Fig. 15). For $x \to 0$ (CdTe), the phonon structure is well resolved. The ZPL of this emission is located at 2.201 eV for $x \to 1$ (ZnTe), but the phonon structure has not changed significantly. The Huang-Rhys factor is $S = 1.6 \pm 0.2$ in ZnTe. In the alloy the phonon structure is smeared out, so neither the phonon coupling nor the ZPL could be determined directly. An estimate of the binding energy E_B of the A centers in the alloys was obtained by subtracting $S(x)\hbar\omega(x)$ from the peak energy. For S and $\hbar\omega$, a linear dependence on the alloy composition ($\hbar\omega = 20.1$ meV in CdTe, $\hbar\omega_{LO} = 26.2$ meV in ZnTe) was assumed. With this assumption the A-center binding energy varies from 127 meV at $x = 0$ to 155 meV at $x = 1$, thus the composition dependence is $E_B(x) = (127 + 28x)$ meV (Fig. 15).

The other emissions in part B of Fig. 14 were determined to be (e, A^0) transitions involving more shallow acceptors (marked as open circles and triangles in Fig. 15). For E_{CdTe}, we obtain 48.0 meV and 58.2 meV, respectively. This points to (e, A^0) transitions involving either an EMT acceptor (e.g., Bell acceptor)[46] or the acceptors N, Li, or Na (see for example Refs. 47 and 48). The binding energy of the two transitions as a function of the composition x is described by $E_B = E_{CdTe} + 8.2x$ meV, with E_{CdTe} the transition energy in CdTe.

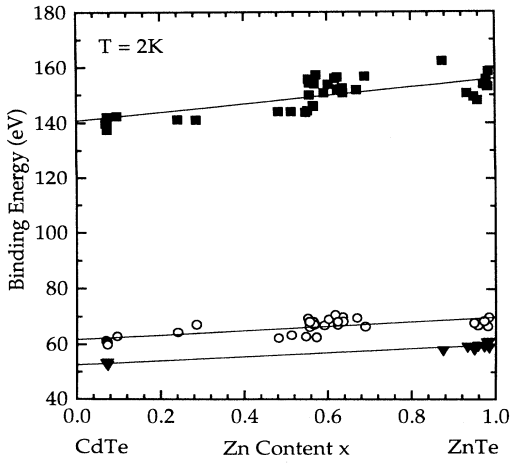

FIG. 15. Binding energy of A centers (full squares), Bell acceptors (Ref. 46) (open circles), and an effective mass type acceptor (full triangles) as a function of the alloy composition x in $Cd_{1-x}Zn_xTe$:Cl.

The third spectral range of interest (labeled as part C in Fig. 14) consists of transitions with an energy of more than 200 meV below band gap. The peak positions as a function of alloy composition are drawn in Fig. 16. For a comparison, the composition dependence of the band gap (solid line) and the A center (closed circles) are drawn. For the band at about 1.05 eV (open circles in Fig. 16, its intensity often dominates the spectrum) the emission energy remains constant over the complete alloy range. This behavior implies that the binding energy increases from CdTe to ZnTe by approximately 800 meV. This PL band has a peak position of (1.11 ± 0.04) eV in CdTe and shifts slightly to lower energy (1.03 ± 0.01) eV in ZnTe. Temperature dependent measurements of this PL band show that it has similar behavior to the previously described 1.135 eV band, i.e., increasing peak energy with increasing temperature. Another emission with a constant peak energy during the composition occurs at a higher Zn content at (0.79 ± 0.02) eV (open squares in Fig. 16). The origin of both emissions is up to now not clear, neither in CdTe nor in ZnTe is a deep defect with a corresponding binding energy identified.

The other two PL bands roughly follow the band-gap dependence in $Cd_{1-x}Zn_xTe$, this results in an almost constant binding energy through the complete alloy from CdTe to ZnTe. The two additional emissions have peak energies at (1.32 ± 0.02) eV in CdTe and (2.08 ± 0.02) eV in ZnTe (full squares), and (1.12 ± 0.04) eV in CdTe and (1.84 ± 0.02) eV in ZnTe (full triangles), respectively. The later was proven to show a similar temperature dependence as the 1.145 eV PL band described in the previous section. The defects being responsible for these PL bands are also not identified.

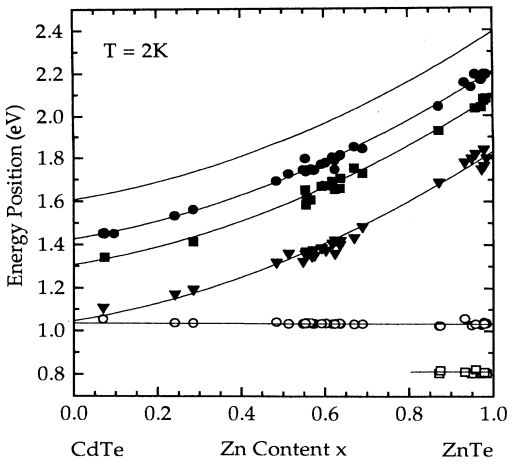

FIG. 16. Energetic positions of the photoluminescence bands in chlorine-doped $Cd_{1-x}Zn_xTe$ as a function of the alloy composition x. Full circles: chlorine A centers, full squares: unknown PL band, full triangles: 1.145 eV PL in CdTe, open circles: 1.135 eV PL in CdTe, open squares: unknown PL band. The upper drawn line gives the band-gap dependence calculated according to Eq. (1), the other drawn lines are guides for the eye.

IV. DISCUSSION

In CdTe, we observed two deep luminescence bands at 1.135 eV and 1.145 eV of unknown origin. The peak position of the 1.135 eV band increases with increasing temperature. The position of the 1.145 eV emission decreases. In the $Cd_{1-x}Zn_xTe$ alloy, these two bands show also opposite behavior. The 1.135 eV band keeps its emission energy independent of the band-gap energy. The 1.145 eV band follows the increase of the band-gap energy.

Often, intrinsic defects such as vacancies on both sublattices are quoted to cause deep defects. We briefly describe the properties of these defects in II-VI compounds, to gain insight as to whether they might be the origin of the observed deep PL bands.

The isolated metal vacancies in ZnS and ZnSe introduced by electron irradiation have well established properties.[49] From EPR and ODMR experiments, the energy level positions as well as the lattice relaxation energies were determined. In Fig. 17, we compare the level positions for ZnS, ZnSe, ZnTe, and CdTe. The metal vacancies act as double acceptors introducing two energy levels in the forbidden gap. In ZnS, the double acceptor level $(2-/-)$ is 1.1 eV above valence band; the single acceptor level $(-/0)$ at $E_{VB}+0.6$ eV. In ZnSe, only the $(2-/-)$ level has been observed at 0.8 eV above valence band. By a comparison with the valence band offset between ZnS and ZnSe, we note that the $(2-/-)$ level roughly follows the valence band as expected for a metal vacancy.

The corresponding A centers in ZnS, ZnSe as well as in the alloy system $ZnS_{1-x}Se_x$ practically parallel the behavior of the $(2-/-)$ level of the isolated vacancy being 0.3 eV lower in energy. In ZnTe the A centers are at E_V+144 meV, in CdTe at E_V+127 meV. The valence band offset between ZnTe and CdTe is very small

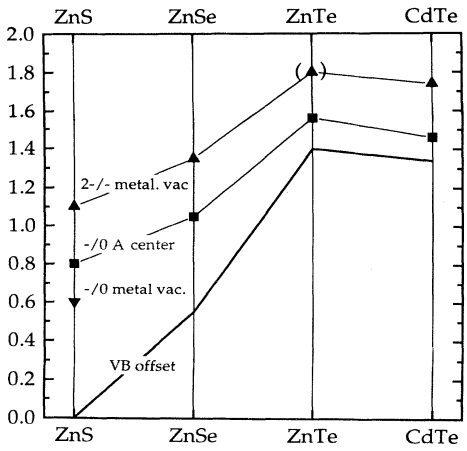

FIG. 17. Comparison of the metal vacancy and level positions in ZnS, ZnSe, ZnTe, and CdTe taking the valence band offsets into account. For details see text.

($\leq$ 60 meV) and since the metal vacancy wave function is dominantly built up by the nearest neighbors Te $5p$ wave functions, which also form the valence band states, the energy level of the A centers should be constant, passing from ZnTe to CdTe. This is indeed observed.

There has been an ongoing discussion about the presence and location of the metal vacancies in ZnTe and CdTe. In ZnTe, no experimental results are available. Assuming that the isolated vacancy level goes parallel with the level of the A centers, the $(2-/-)$ of V_{Zn} in ZnTe should be at $E_{VB}+0.40$ eV, and following the arguments outlined above, approximately at an equal position in CdTe. Our recent photo-EPR investigation on V_{Cd} in CdTe[14] arrived with the same conclusion. In EPR, the negative charged state of the vacancy is monitored. Illumination with light of energy less than half of the band gap down to 0.4 eV decreased the EPR signal, due to the ionization transition $V_{Cd}^{-} \rightarrow V_{Cd}^{2-} + h_{VB}^{+}$.

In bulk ZnS, ZnSe, and ZnTe the isolated vacancies have not been observed in as grown crystals, electron irradiation was necessary to create them (ZnS, ZnSe).[49] In CdTe purification and special thermal treatments were necessary to have at most 10^{16} cm^{-3} isolated V_{Cd} present.[14] This observation does not speak against a low abundance of the metal vacancies in as-grown crystals, but rather to the high residual impurity concentrations in these II-VI compounds. Ag and Cu, both frequently present in concentrations up to 10^{17} cm^{-3}, occupy metal sites (Ag diffuses even at room temperature), and hence isolated vacancies are expected to be a minority species.

According to our experimental findings the metal vacancy in CdTe induces only one level $(2-/-)$ in the gap. If the $(-/0)$ acceptor level falls within the band gap it should be shallow. Taking as a reference the separation between the $(2-/-)$ and $(-/0)$ levels in ZnS which is of the order of 0.5 eV it is inside the valence band, probably also in ZnTe. From the behavior of the A centers in ZnS, ZnSe, ZnTe, and CdTe, we conclude that the isolated vacancy level $(2-/-)$ in ZnTe is located not more than 400 meV above valence band as it is in CdTe.

The incorporation of A centers in CdTe depends on the nature of the dopant used. Chlorine doping results in highly resistive material, the ratio of isolated donors Cl_{Te} and A centers can be as high as $1:1$.[50] This is in contrast with In doping where the fraction of A centers formed is much less easily leading to n-type material.[21] The control of the stoichiometry, the residual impurity content as well as choosing the proper dopant atom should lead to n-type conductivity in ZnTe as indeed demonstrated just recently.[5]

The deep luminescence bands in $Cd_{1-x}Zn_xTe$ fall into two classes, one which has constant energy separation with respect to the valence band and another one which follows the conduction band. The 1.135 eV band has a constant PL energy in $Cd_{1-x}Zn_xTe$ and shows increasing PL energy with increasing temperature. It thus can originate from an internal recombination of a transition metal element (in Ref. 41 it was argued to be caused by an internal recombination of iron) or an internal recombination on the metal vacancy. The photo-EPR results gave as an upper limit for the $2-/-$ level $E_B < 0.4$ eV.

A level at $E_V + 0.318$ eV is often observed in electrical measurements (see for example Ref. 51) and assigned to a hole trap (in Vul *et al.*[52] to the V_{Cd}^{-0} level). The cross section with 1.5×10^{-14} cm^2 is not inconsistent with a deep intrinsic impurity.

The 1.145 eV band follows the conduction band shift. Such behavior can be expected for a native vacancy on the anion sublattice, as the nearest neighbor ions are completely exchanged in the alloy from CdTe to ZnTe. The binding energy of the 1.145 eV band is $E_B = (280 \pm 15)$ meV. Photo-EPR located the Te vacancy (0/+) level at $E_{VB} + 0.2$ eV, which may give evidence that this defect is involved in the recombination of the 1.145 eV band.

There has been a tremendous scatter on energy level positions and possible identifications for intrinsic and extrinsic defects in ZnTe and CdTe. It is now clear from our work and the work of Pautrat *et al.*[2] and Dean[53] that for the common extrinsic residual impurities, Cu has the largest binding energy of 140 meV (we neglect Au which is not found in as grown crystals). The more shallow acceptors are P_{Te} and As_{Te}. In Cl-doped CdTe, an additional acceptor appears with a binding energy below the effective mass limit.[46] It is speculated to be due to a Cl_{Te}^{+}–V_{Cd}^{2-}–Cl_{Te}^{+} defect,[46] but a clear microscopic identification is still missing. In a recent investigation combining positron annihilation spectroscopy and PL, it became evident that at very high doping concentration the recombination with the 44 meV acceptor becomes prominent. Also, a new vacancy related signal appears in the positron spectroscopy at high doping concentrations. More details will be presented elsewhere.[54] Energy levels at 50 meV and 150 meV above valence band were originally identified with the two ionization states of a native double acceptor. Later on it became clear that they belong to the two acceptors P_{Te} and Cu_{Cd}.[47,26] Cu_{Cd} has practically the identical binding energy in CdTe and ZnTe. *A* centers have a very similar binding energy in both compounds and due to the lack of a clear spectroscopic identification the presence of *A* centers was therefore questioned for a long time.

To predict the energy levels of the V_{Zn}^{2-} and V_{Cd}^{2-} from the *A*-center binding energy, a simple donor-acceptor-pair interaction relation, which worked for deep donor-acceptor complexes in GaP (Ref. 55) has been used. The energy levels of V_{Zn}^{2-} (V_{Cd}^{2-}) should be of the order of 750 meV if the *A*-center binding energy is of the order of (200 ± 50) meV.[56,57] At least for CdTe these predictions do not hold, possibly also not for ZnTe. The dominant species in Cl-doped $Cd_{1-x}Zn_xTe$ are *A* centers with binding energies of 127 meV (155 meV in ZnTe). The double acceptor level for V_{Cd} is clearly below 400 meV and not at midgap and we do not expect it to be much deeper in ZnTe. Our investigations in CdTe with ODMR and the PL study in $Cd_{1-x}Zn_xTe$ confirms the results from ODMR on Cl- and Al-doped ZnTe by Bittebierre and Cox.[19] The magnetic resonance data have very similar characteristics (see Table III) with respect to g values and hyperfine interaction constants.

It still remains a puzzle, why CdTe doped with Cl is highly resistive due to the balance of two shallow defects, the isolated Cl donor with $E_B = 14$ meV and shallow acceptors (*A* centers) with $E_B = 120$ meV and the additional presence of residual acceptors (P_{Te}, Cu_{Cd}) in the concentration range up to 10^{17} cm^{-3}. Resistivities as high as 10^{10} Ω cm are currently reported,[58] i.e., the Fermi level is pinned to midgap. Vanadium-doped CdTe also produces highly resistive material,[59] where the *V* donor level is predicted to be close to midgap. It appears that there is still a deep donor missing to explain the compensation behavior of doped CdTe. Intrinsic donors as antisites or Cd interstitials could be candidates. In this context, it is worth noting that CdTe and $Cd_{1-x}Zn_xTe$ can be grown highly resistive without any doping by a high pressure technique.[60]

V. SUMMARY

To characterize the defects and residual impurities in undoped and donor doped CdTe and $Cd_{1-x}Zn_xTe$ infrared absorption spectroscopy, photoluminescence and optically detected magnetic resonance have been used. Infrared absorption is the most specific tool to characterize the residual acceptors such as Cu and Ag. The PL properties of the V_{Cd}-donor complexes (*A* centers) have been studied for different donor species involved in the complex.

In addition to these defects, photoluminescence bands located at 1.145 eV and at 1.135 eV in CdTe were observed. They show distinct differences in the temperature dependent PL: The peak energy of the 1.135 eV band increases with temperature, the peak energy of the 1.145 eV band decreases. The latter gives evidence for a band to defect recombination, whereas the behavior of the 1.135 eV emission is characteristic for an internal recombination. Investigating the luminescence band present in the $Cd_{1-x}Zn_xTe$ alloy system, we found that the 1.135 eV luminescence keeps its emission energy through the complete alloy, and the 1.145 eV PL energy increases as the band gap does.

Spectroscopically, the defects responsible for both PL bands have not been identified so far. But summarizing the results on vacancies in II-VI semiconductors, some arguments are found that these defects might be involved.

ACKNOWLEDGMENT

The work was supported in great extent by the German Research Council DFG.

[1] S.S. Devlin, in *Physics and Chemistry of II-VI Compounds*, edited by M. Aven and J.S. Prener (North-Holland, Amsterdam, 1967), p. 552ff.
[2] J.L. Pautrat, J.M. Francou, N. Magnea, E. Molva, and K. Saminadayar, J. Cryst. Growth **72**, 194 (1985).
[3] R.M. Park, M.B. Troffer, C.M. Rouleau, J.M. DePuydt, and M.A. Haase, Appl. Phys. Lett. **57**, 2127 (1990).
[4] D. Hommel, A. Waag, S. Scholl, and G. Landwehr, Appl. Phys. Lett. **61**, 1546 (1992).
[5] I.W. Tao, M. Jurkovic, and W.I. Wang, Appl. Phys. Lett. **64**, 1848 (1994).
[6] G. Mandel, Phys. Rev. **134**, A1073 (1964).
[7] R.S. Title, F. Morehead, and G. Mandel, Phys. Rev. **136**, A300 (1964).
[8] G. Mandel, F. Morehead, and P.R. Wagner, Phys. Rev. **136**, A826 (1964).
[9] F.F. Morehead and G. Mandel, Phys. Rev. **137**, A924 (1965).
[10] D.B. Laks, C.G. Van de Walle, G.F. Neumark, and S.T. Pantelides, Phys. Rev. Lett. **66**, 648 (1991).
[11] G.F. Neumark, Phys. Rev. Lett. **62**, 1800 (1989).
[12] C.G. Van de Walle, D.B. Laks, G.F. Neumark, and S.T. Pantelides, Phys. Rev. B **47**, 9425 (1993).
[13] D.B. Laks, C.G. Van de Walle, G.F. Neumark, and S.T. Pantelides, Appl. Phys. Lett. **63**, 1375 (1993).
[14] P. Emanuelsson, P. Omling, B.K. Meyer, M. Schenk, and M. Wienecke, Phys. Rev. B **47**, 15 578 (1993).
[15] B.K. Meyer, P. Omling, E. Weigel, and G. Müller-Vogt, Phys. Rev. B **46**, 15 135 (1992).
[16] D.M. Hofmann, P. Omling, H.G. Grimmeiss, B.K. Meyer, K.W. Benz, and D. Sinerius, Phys. Rev. B **45**, 6247 (1992).
[17] W. Stadler, B.K. Meyer, D.M. Hofmann, B. Kowalski, P. Emanuelsson, P. Omling, E. Weigel, G. Müller-Vogt, and R.T. Cox, Mater. Sci. Forum. **143-147**, 399 (1994).
[18] C.B. Norris and C.E. Barnes, Rev. Phys. Appl. **12**, 219 (1977).
[19] J. Bittebierre and R.T. Cox, Phys. Rev. B **34**, 2360 (1986).
[20] D. Sinerius, Ph.D. thesis, University of Freiburg, 1992.
[21] E. Weigel, Ph.D. thesis, University of Karlsruhe, 1993.
[22] J.L. Reno and E.D. Jones, Phys. Rev. B **45**, 1440 (1992).
[23] P. Rudolph and M. Mühlberg, Mater. Sci. Eng. B **16**, 8 (1993).
[24] E. Weigel, G. Müller-Vogt, B. Steinbach, W. Wendl, W. Stadler, D.M. Hofmann, and B.K. Meyer, Mater. Sci. Eng. B **16**, 17 (1993).
[25] E. Molva, J.P. Chamonal, G. Milchberg, K. Saminadayar, B. Pajot, and G. Neu, Solid State Commun. **44**, 351 (1982).
[26] J.P. Chamonal, E. Molva, and J.L. Pautrat, Solid State Commun. **43**, 801 (1982).
[27] A. Baldereschi and N.O. Lipari, Phys. Rev. B **9**, 1525 (1974).
[28] K. Saminadayar, N. Magnea, J.L. Pautrat, and B. Pajot, Phys. Status Solidi B **106**, 215 (1981).
[29] E. Molva, J.P. Chamonal, and J.L. Pautrat, Phys. Status Solidi B **109**, 635 (1982).
[30] P. Baeume, F. Kubacki, and J. Gutowski, J. Cryst. Growth **138**, 266 (1994).
[31] C. Onodera and T. Taguchi, J. Cryst. Growth **101**, 502 (1990).
[32] K. Zanio, in *Cadmium Telluride*, edited by R.K. Willardson and A.C. Beer, Semiconductors and Semimetals Vol. 13 (Academic, New York, 1972).
[33] J.M. Francou, K. Saminadayar, and J.L. Pautrat, Phys. Rev. B **41**, 12 035 (1990).
[34] J. Camasset, D. Auvergne, H. Mathieu, R. Triboulet, and M. Varfainy, Solid State Commun. **13**, 63 (1973).
[35] S. Biernacki, U. Scherz, and B.K. Meyer, Phys. Rev. B **48**, 11 726 (1993).
[36] D.G. Thomas, J.J. Hopfield, and W.M. Augustyniak, Phys. Rev. **140**, A202 (1965).
[37] K. Zanio, J. Electron. Mater. **3**, 327 (1974).
[38] S. Iida, J. Phys. Jpn. **25**, 177 (1968).
[39] G.E. Pake and T.E. Estle, *The Physical Principles of Electron Paramagnetic Resonance* (Benjamin, London, 1973).
[40] J.E. Nicholls, J.J. Davies, N.R. Poolton, R. Mach, and G.O Müller, J. Phys. C **18**, 455 (1985).
[41] K. Lischka, G. Brunnthaler, and W. Jantsch, J. Cryst. Growth **72**, 335 (1985).
[42] R.C. Bowman and D.E. Cooper, Appl. Phys. Lett. **53**, 1521 (1988).
[43] D.B. Fitchen, in *Physics of Color Centers*, edited by W.B. Fowler (Academic, New York, 1968), p. 294ff.
[44] S. Shionoya, T. Koda, K. Era, and H. Fujiwara, J. Phys. Soc. Jpn. **19**, 1157 (1964).
[45] A. Doernen, W. Stadler, D.M. Hofmann, and B.K. Meyer (unpublished).
[46] R.O. Bell, Solid State Commun. **16**, 913 (1975).
[47] E. Molva, K. Saminadayar, J.L. Pautrat, and E. Ligeon, Solid State Commun. **48**, 955 (1983).
[48] E. Molva, J.L. Pautrat, K. Saminadayar, G. Milchberg, and N. Magnea, Phys. Rev. B **30**, 3344 (1984).
[49] G.D. Watkins (unpublished).
[50] B.K. Meyer (unpublished).
[51] A.A. Grippius, J.R. Panossian, and V.A. Chapnin, Phys. Status Solidi A **21**, 753 (1974).
[52] B.M. Vul, V.S. Ivanov, V.A. Rukavishnikov, V.M. Sal'man, and V.A. Chapnin, Fiz. Tekh. Poluprovodn. **6**, 1264 (1972) [Sov. Phys. Semicond. **6**, 1106 (1973)].
[53] P.J. Dean, H. Venghaus, J.C. Pfister, B. Schaub, and J. Marine, J. Lumin. **16**, 363 (1978).
[54] R. Krause-Rehberg, A. Polity, Th. Abgarjan, W. Stadler, D.M. Hofmann, B.K. Meyer, and M. Azoulay (unpublished).
[55] P.J. Dean, in *Deep Centers in Semiconductors*, edited by S.T. Pantelides (Gordon and Breach, New York, 1986).
[56] T. Taguchi, Phys. Status Solidi B **96**, K33 (1979).
[57] P. Höschl, P. Polívka, V. Prosser, M. Vaněček, and M. Skřiváková, Rev. Phys. Appl. **12**, 229 (1977).
[58] B. Biglari, M. Samlmi, J.M. Koebel, M. Hage-Ali, and P. Siffert, Phys. Status Solidi A **100**, 589 (1987).
[59] A. Partovi, J. Millerd, E.M. Garmire, M. Ziari, W.H. Steier, S.B. Trivedi, and M.B. Klein, Appl. Phys. Lett. **57**, 846 (1990).
[60] F.P. Doty, J.F. Butler, J. Schetzina, and K.A. Bowser, J. Vac. Sci. Technol. **10**, 1418 (1992).